ELSEVIER

Applied Catalysis A: General 234 (2002) 55–64

APPLIED CATALYSIS A: GENERAL

www.elsevier.com/locate/apcata

Preparation of high loading silica-supported nickel catalyst: analysis of the reduction step

Daniel L. Bhering, Márcio Nele, José Carlos Pinto, Vera M.M. Salim*

Programa de Engenharia Química, COPPE, Universidade Federal do Rio de Janeiro, Centro de Tecnologia, Cidade Universitária, Bloco G, Sala 115, Caixa Postal 68502, CEP 21945 Rio de Janeiro, Brazil

Received 2 October 2001; received in revised form 6 March 2002; accepted 10 March 2002

Abstract

The reduction step used for preparation of high loading silica-supported nickel (Ni/SiO_2) catalysts was analyzed with the help of statistical experimental design. Two catalyst precursors prepared by deposition–precipitation (DP) method and presenting significantly different metal–support interactions were studied. Empirical models were developed for the degree of reduction and for the metallic area of the Ni/SiO_2 catalysts as functions of the reduction variables (final reduction temperature, heating rate, flow rate and hydrogen concentration of the reducing mixture) for each precursor. For the precursor with low nickel–support interaction, high degrees of reduction were attained regardless of the reducing conditions used; however, operation conditions exerted a significant influence upon the final catalyst metallic area. For the precursor with high nickel–support interaction, both the degree of reduction and the final catalyst metallic area were strongly affected by the reducing conditions. The reducing conditions were then optimized for both catalyst precursors in order to maximize the final catalyst metallic area. Simulation results were validated experimentally and indicated that optimum reducing conditions may depend significantly on the nature of the catalyst precursor. Finally, a mixed model was built by the linear combination of the two original models, allowing the successful optimization of the reducing conditions for a precursor with intermediate nickel–support interaction. These results suggest that reducing conditions may be tuned at plant site as a function of the metal–support interaction of catalyst precursors, with the aid of mathematical models built for model catalyst precursors.

Keywords: Nickel catalyst; Reduction; Experimental design; Silica-supported catalyst

1. Introduction

The optimization of the catalyst preparation steps is still a field of intense research [1–4]. The catalyst preparation steps involve several simultaneous physicochemical processes that are not well understood and the search for more economically/environmentally efficient catalysts drives the continuous research in the area. Empirical and phenomenological mathematical models can be used as tools for optimization of the final catalyst properties and fine-tuning of the preparation variables because they can describe quantitatively how the preparation conditions and catalyst properties are related.

Hydrogenation reactions are of major importance in the chemical industry. For example, more than 90% of the catalytic production processes of Ciba Geigy (now Novartis) in 1996 were hydrogenations, most of them using silica-supported nickel (Ni/SiO_2) catalysts. Not surprisingly, these catalysts have been intensively studied in the open literature. Particularly, the works

* Corresponding author.
E-mail address: vera@peq.coppe.ufrj.br (V.M.M. Salim).

0926-860X/02/$ – see front matter
PII: S0926-860X(02)00198-9

developed by Schuit and van Reijen [1], Coenen and Linsen [2], Geus et al. [3] and Hermans and Geus [4] may be regarded as fundamental landmarks in this field. More recent works analyze the effect of additives (Ca, Ba) and aging upon the final catalyst properties [5]; study the preparation of catalysts with controlled pore structure [6]; analyze the fundamental relations between the nature of the nickel-deposited phase and the catalyst textural properties [7,8]; propose a method to improve the nickel oxide dispersion on the silica by silica-pillared phosphates [9]; analyze the influence of the carrier textural properties, nickel loading, precipitating agent and the precipitation and aging steps on the metallic dispersion and metal–silica interaction [10–13]. Particularly, the influence of the precipitation and aging steps upon the final catalyst properties was analyzed simultaneously with the help of statistical methods [14]. It was found that catalyst aging is an effective method to control the extent of the nickel–support interaction, the metallic area and the textural catalyst properties. Optimal precipitation and aging conditions were then proposed.

Recently, efforts have been concentrated on understanding the relationships among the preparative conditions, the properties of the precursor phases formed and the reducibility of the precursors [15–18] using the "change one factor at a time method". Particularly, Burattin et al. [19] investigated the influence of the reduction conditions on the size of the metal particles and on the extent of reduction and proposed a mechanism of formation of metal particles for catalyst samples prepared by deposition–precipitation (DP) method. However, these studies have not been focused upon the optimization of the final catalyst properties.

In a previous study [14], models developed to describe the precipitation and aging steps were used to optimize the precursor preparation in respect to the metallic area of the reduced nickel, when precursors were subject to standard reduction conditions. In this communication, the influence of the reduction step upon the final catalyst properties is investigated to allow the maximization of the final catalyst metallic area. In order to do that, two Ni/SiO_2 precursors presenting significantly different degrees of nickel–silica interaction were prepared using the preparative method previously developed [10,11]. The reducing variables analyzed were final reduction temperature, heating rate and flow rate and hydrogen concentration of the reducing mixture. The effects of all operation conditions were investigated simultaneously using statistical design of experiments, in order to determine the relative importance of each variable, identify possible variable interactions and optimize the reducing conditions, allowing the development of a reducing recipe that maximize the catalyst efficiency.

2. Experimental

2.1. Catalysts preparation

Catalyst precursors were prepared through DP method at 363 K, using $NaHCO_3$ (0.8 M) as the precipitating agent, FC celite–manville (1% alumina, 42 m^2/g and $V_p = 1.1\ cm^3/g$) as the carrier and nickel nitrate solution (0.8 M) as the metal source. Precursors were aged at 363 K for different aging times [14]. Two precursors with very different metal–support characteristics were selected for this study. The nomenclature ($iNi_{j\text{-}k\text{-}l}$) used here is similar to the one used previously [14], where i is the nickel content (wt.%), j the precipitation temperature (K), k the aging temperature (K) and l the aging time (h).

The precursor $40Ni_{363\text{-}363\text{-}0}$ (45 m^2/g and 37 wt.% Ni) is formed basically by supported NiO and presents a low metal–support interaction. The precursor $40Ni_{363\text{-}363\text{-}20}$ (325 m^2/g and 42 wt.% Ni) is formed predominantly by nickel silicate (antigorite) and presents significant metal–support interaction [4,14]. Fig. 1 shows the typical TPR profiles obtained at the same conditions ($\beta = 5$ K/min; $C_{H_2} = 1.7\%$, $F_{H_2} = 50\ cm^3/min$ and $T_f = 1075$ K).

2.2. Analysis of reduction step

The reducibility was evaluated with an ordinary temperature-programmed reduction (TPR) piece of equipment. Different final reducing temperatures were used for each catalyst precursor in order to guarantee adequate degree of reduction and minimum sintering. The final reduction temperature was kept constant for 20 min before the interruption of the reduction experiment in all cases.

The hydrogen uptake observed during the TPR was expressed as the reduction degree (%R), assuming that the transition observed is Ni^{2+} to Ni^0. At the end of the

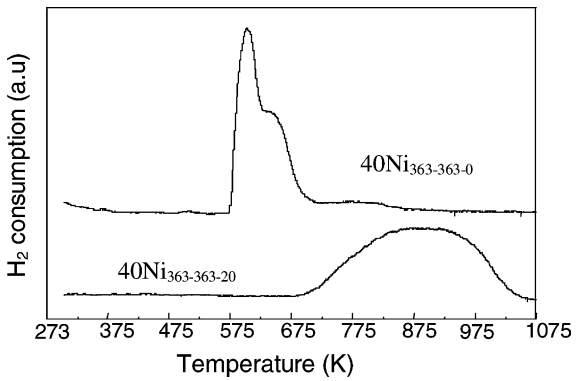

Fig. 1. TPR profiles of the $40Ni_{363\text{-}363\text{-}0}$ and $40Ni_{363\text{-}363\text{-}20}$ precursors ($\beta = 5$ K/min, $C_{H_2} = 1.7\%$, $F_{H_2} = 50\,cm^3$/min and $T_f = 1075$ K).

TPR experiment, the metallic dispersion was measured based on the adsorption and desorption peaks obtained by quickly cooling (823 K down to room temperature) and heating (room temperature up to 773 K) of the reduced sample in H_2/Ar mixture (heating/cooling rates of 100 K/min). Nickel metallic areas were calculated assuming a stoichiometry of ^{1}H/surface nickel at room temperature. The geometric area of a surface nickel atom was taken as 6.3 Å^2 [5]. The nickel area (S^0_{Ni}) is referred to the reduced nickel.

2.3. Experimental design

The main variable effects and the variable interactions were investigated by using a Taguchi experimental design [14,20] and the list of variables analyzed is shown in Table 1. In short, a Taguchi design is an ordered fraction of the full factorial design, which allows the estimation of the parameters of Eq. (1) with maximum precision. The matrix of experiments was designed for four variables and contained eight experiments, as shown in Table 2 (experimental conditions are normalized in the range [−1,+1]). Additionally, four replicates (experiments 9–12) were performed at the central point in order to evaluate the experimental error (Table 2). Experimental conditions were selected in order to allow the computation of the main variable effects (a_{ii} in Eq. (1)) and the variable interactions (a_{ij} in Eq. (1)) in simple polynomial models (Eq. (1)). However, as some variable interactions are confounded (cannot be estimated independently), additional experiments may be necessary for discrimination of important variable interaction effects. The use of statistical experimental design in catalyst preparation is thoroughly discussed elsewhere [14].

Table 2
Matrix of experiments

Experiment	Run order	β^*	$F^*_{H_2}$	T^*_f	$C^*_{H_2}$
1	4	−1	−1	−1	−1
2	7	−1	−1	+1	+1
3	9	−1	+1	−1	+1
4	2	−1	+1	+1	−1
5	12	+1	−1	−1	+1
6	1	+1	−1	+1	−1
7	3	+1	+1	−1	−1
8	6	+1	+1	+1	+1
9–12	5–11	0	0	0	0

The final catalyst properties regarded as relevant for evaluation of the performance of the reduction procedure were reducibility (%R) and metallic surface per gram of nickel (S_{Ni}). These variables (hereafter called responses) were correlated with the reduction variables through linear regression analysis.

Table 1
Real and coded values of the experimental variables

Variable	Coded variable	Lower value (−1)	Central value (0)	Upper value (+1)
Heating rate (K/min)	β^*	5	10	15
H_2/Ar gas flow rate (cm^3/min)	$F^*_{H_2}$	20	35	50
Final reduction temperature (K)	T^*_f	773[a]	923[a]	1073[a]
		873[b]	998[b]	1123[b]
H_2/Ar gas concentration (% (v/v))	$C^*_{H_2}$	1.7	5.1	10.0

[a] Condition for the $40Ni_{363\text{-}363\text{-}0}$ precursor.
[b] Condition for the $40Ni_{363\text{-}363\text{-}20}$ precursor.

3. Results and discussion

The experimental results (responses) for the reducibility tests obtained for the non-aged ($40Ni_{363\text{-}363\text{-}0}$) and aged ($40Ni_{363\text{-}363\text{-}20}$) precursors are shown in Tables 3 and 4, respectively. The reduction conditions are labeled in the form $iR_{j\text{-}k\text{-}l}$, where i is the heating rate (β, K/min), j the final temperature (T_f, K), k the H_2/Ar flow rate (F_{H_2}, cm^3/min) and l the H_2/Ar gas concentration (C_{H_2}, vol%). Tables 3 and 4 show that the set of reducing conditions analyzed gives birth to materials with very different properties, especially regarding the metallic surface area.

Catalysts obtained from the non-aged precursor ($40Ni_{363\text{-}363\text{-}0}$) presented high degree of reducibility in all operation conditions, ranging from 95.5 to 101.6%. These results show that the reduction of the NiO phase is not significantly influenced by the reduction variables within the analyzed experimental range. The precursors are reduced almost completely even at mild reduction conditions (e.g. all the variables at their lower levels). This result is supported by the TPR profile shown in Fig. 1, where it may be seen that this precursor is completely reduced at approximately 750 K. In spite of that, the metallic surface area depended strongly upon the reducing conditions.

Table 3
Experimental results for the $40Ni_{363\text{-}363\text{-}0}$ precursor[a]

Number	Reduction	Response	
		%R	S_{Ni} (m^2/g Ni)
1	$5R_{773\text{-}20\text{-}1.7}$	98.8	18.3
2	$5R_{1073\text{-}20\text{-}10}$	95.5	9.1
3	$5R_{773\text{-}50\text{-}10}$	100.6	27.9
4	$5R_{1073\text{-}50\text{-}1.7}$	100.0	6.0
5	$15R_{773\text{-}20\text{-}10}$	101.6	22.0
6	$15R_{1073\text{-}20\text{-}1.7}$	100.1	10.3
7	$15R_{773\text{-}50\text{-}1.7}$	99.5	33.8
8	$15R_{1023\text{-}50\text{-}10}$	100.7	15.2
9	$10R_{923\text{-}35\text{-}5.1}$	99.2	21.3
10	$10R_{923\text{-}35\text{-}5.1}$	97.3	19.0
11	$10R_{923\text{-}35\text{-}5.1}$	98.5	20.4
12	$10R_{923\text{-}35\text{-}5.1}$	99.0	19.8
Maximum		101.6	33.8
Mean		99.2	18.6
Minimum		95.5	6.0

[a] $iR_{j\text{-}k\text{-}l}$: i is the heating rate (β), j the final temperature (T_f), k the H_2/Ar flow rate (F_{H_2}) and l the H_2/Ar gas concentration (C_{H_2}).

Table 4
Experimental results for the $40Ni_{363\text{-}363\text{-}20}$ precursor[a]

Number	Reduction	Response	
		%R	S_{Ni} (m^2/g Ni)
1	$5R_{873\text{-}20\text{-}1.7}$	53.3	21.6
2	$5R_{1123\text{-}20\text{-}10}$	89.4	38.4
3	$5R_{873\text{-}50\text{-}10}$	95.8	87.1
4	$5R_{1123\text{-}50\text{-}1.7}$	94.9	43.6
5	$15R_{873\text{-}20\text{-}10}$	73.1	42.9
6	$15R_{1123\text{-}20\text{-}1.7}$	101.4	22.8
7	$15R_{873\text{-}50\text{-}1.7}$	61.9	39.7
8	$15R_{1023\text{-}50\text{-}10}$	101.0	47.3
9	$10R_{998\text{-}35\text{-}5.1}$	94.5	44.0
10	$10R_{998\text{-}35\text{-}5.1}$	93.3	46.7
11	$10R_{998\text{-}35\text{-}5.1}$	93.5	44.6
12	$10R_{998\text{-}35\text{-}5.1}$	95.0	45.2
Maximum		101.4	87.1
Mean		79.5	43.7
Minimum		53.3	21.6

[a] $iR_{j\text{-}k\text{-}l}$: i is the heating rate (β), j the final temperature (T_f), k the H_2/Ar flow rate ($F^*_{H_2}$) and l the H_2/Ar gas concentration ($C^*_{H_2}$).

A wide range of metallic surface area (6.0–33.8 m^2/g Ni) was obtained, which emphasizes that the choice of the reduction conditions is very important for proper control of the sintering of the metallic nickel particles.

Both the degree of reduction and the reducibility of the aged precursor ($40Ni_{363\text{-}363\text{-}20}$), in contrast, are very sensitive to the reduction conditions (Table 4). As shown in Fig. 1, these catalysts can be completely reduced only at very high temperatures (998 K), which may have a deleterious effect on the metallic area, depending on the levels of the remaining reduction conditions. Therefore, the proper choice of the reducing conditions of this precursor is even more difficult.

Based on the available experimental data, it is possible to evaluate the importance of each variable effect and respective interactions quantitatively. This can be performed by assuming that the experimental responses (degree of reduction and metallic area) depend on the normalized reduction variables as shown in Eq. (1),

$$y = b + \sum_{i=1}^{n} a_{ii}x_i + \sum_{i=1}^{n}\sum_{j=2,\, j>i}^{n} a_{ij}x_i x_j \qquad (1)$$

where x_i are the independent variables (β^*, $F^*_{H_2}$, T^*_f, $C^*_{H_2}$), b the independent polynomial coefficient, a_{ii}

the main effect of variable i and a_{ij} the interaction effect between the variables i and j. The polynomial coefficients (and respective errors) can be evaluated using standard linear least-squares procedures [20]. If the coefficient error is of the same order of magnitude of the respective coefficient, then the polynomial coefficient may be discarded based on a statistical test of significance (e.g. Student's t-test). The degree of significance used throughout this manuscript was set to 95%.

If Eq. (1) is used to fit the experimental data presented in Tables 3 and 4, one will find that some interactions are confounded and cannot be evaluated independently. This means that some interactions (for instance, $C^*_{H_2} \cdot T^*_f$ and $\beta^* \cdot F^*_{H_2}$) assume the same values throughout the experimental design matrix. As a result, when the linear regression is performed the terms $C^*_{H_2} \cdot T^*_f$ and $\beta^* \cdot F^*_{H_2}$ have the same coefficient (a_{ij}'s) and one is not able to determine if the estimated coefficient (a_{ij}) belongs to $C^*_{H_2} \cdot T^*_f$ or $\beta^* \cdot F^*_{H_2}$. So, it is impossible to find out which one of the interactions is really important based solely on the experimental data and on the model. In these cases, it may be necessary to perform additional discrimination procedures. A more detailed discussion about confounding in design of experiments can be found elsewhere [20].

Initially, the NiO rich precursor ($40Ni_{363\text{-}363\text{-}0}$) was analyzed. Eqs. (2) and (3) show how the degree of reduction and the metallic area per gram of nickel depend on the analyzed operation variables.

$$\%R = 99.3 \pm 0.5 \tag{2}$$

$$S_{Ni} = (19.0 \pm 1.0) - (7.7 \pm 1.1)T^*_f + (2.9 \pm 1.1)F^*_{H_2} + (2.8 \pm 1.2)\beta^* \tag{3}$$

Eq. (2) shows that the operation variables do not affect the degree of reduction within the experimental range investigated and that the degree of reduction obtained within the investigated experimental region may be assumed to be constant with confidence of 95%. This was already expected since the catalyst was completely (or almost completely) reduced in all experiments. Therefore, an average degree of reduction can represent the experimental data properly without any additional correction for any variable effect.

Regarding the metallic area, Eq. (3) shows that the most important variable effect is the final reduction temperature. As the final reduction temperature increases, the catalyst metallic area decreases due to nickel sinterization [21]. The heating rate and the gas flow rate also exert a direct effect on the final catalyst metallic area per gram of nickel. The effect of the heating rate may be related to the shorter reduction time, which reduces the time available for metallic nickel agglomeration and/or to the formation of more metallic nickel (and consequently smaller) seeds, as reduction temperature increases faster. In both cases, the metallic area is expected to increase, as observed experimentally. The effect of the gas flow rate can be attributed to the more efficient heat and water removal from the catalyst [22], which leads to lower rates of nickel agglomeration. The hydrogen concentration does not exert any significant influence upon the metallic area of this precursor.

Although none of the variable interaction effects were significant within the 95% confidence level set before, the interaction between the final reduction temperature and the gas flow rate was 93% significant and the inclusion of this interaction into the model (Eq. (3)) increased the linear regression correlation coefficient from 0.92 to 0.97. In order to confirm the importance of this interaction factor, two extra experiments were performed and model predictions for the metallic area were compared to the values obtained experimentally for both models obtained: with and without the interaction term.

The two designed experiments maximize the effect of the variable interaction upon the metallic area in the analyzed experimental grid and are not confounded with the other remaining model effects. Therefore, the designed experiments maximize the model discrimination capacity. The results obtained are shown in Table 5.

Table 5 shows that the interaction term improves the predictive capacity of the model significantly and that this interaction must be taken into account. Physically,

Table 5
Experiments for the evaluation of the importance of the interaction term $F^*_{H_2} \cdot T^*_f$ in Eq. (4)

Number	Reduction	S_{Ni} (m^2/g Ni)		
		Eq. (3) prediction	Eq. (4) prediction	Experimental
13	$5R_{773\text{-}50\text{-}1.7}$	26.6	24.1	22.1
14	$15R_{773\text{-}20\text{-}1.7}$	26.7	29.3	30.9

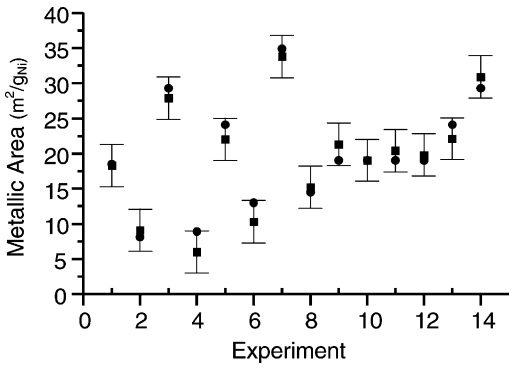

Fig. 2. Comparison between observed (■) and predicted metallic area (●) for the $40Ni_{363\text{-}363\text{-}0}$ precursor.

this term may be related to the rate of water removal during the reduction reaction. This may be especially true at lower temperatures ($T^* = -1$), where the use of a higher gas flow rate ($F^*_{H_2} = +1$) probably increases the water removal rate from the surface, as the diffusivity of the water is lower at lower temperature and it guarantees a more efficient reduction. Eq. (4) presents the empirical model for the metallic area per gram of nickel, including the interaction effect.

$$S_{Ni} = (19.0 \pm 1.0) + (2.8 \pm 1.2)\beta^* + (2.9 \pm 1.1)F^*_{H_2} - (7.7 \pm 1.1)T^*_f - (2.5 \pm 1.1)F^*_{H_2} \cdot T^*_f \quad (4)$$

The excellent agreement between the model and the experimental results can be seen in Fig. 2. The error bars were calculated based on the results obtained from replicated experiments at the central point. Errors were assumed to be constant throughout the experimental region.

Eq. (4) was used to find the reducing conditions that would lead to maximum metallic area per gram of nickel. Analyzing Eq. (4), it is possible to conclude that the optimum operation conditions are $\beta^* = +1$, $F^*_{H_2} = +1$ and $T^*_f = -1$. This optimum condition, hereafter called R_{Ox}, is part of the original experimental matrix (experimental condition 7 of Table 2). At these conditions, Table 3 shows that the experimental metallic area obtained experimentally was equal to $S_{Ni} = 33.8\,m^2/g$ Ni about 20% larger than the second best result obtained for experimental condition 3 ($S_{Ni} = 27.9\,m^2/g$ Ni).

Similar regression procedures were applied to the aged precursor ($40Ni_{363\text{-}363\text{-}20}$). Due to confounding, there are two different equations that are equally able to fit the experimental metallic area data, as shown in Eqs. (5) and (6),

$$S_{Ni} = (44.3 \pm 2.0) + (12.4 \pm 2.4)F^*_{H_2} - (5.1 \pm 2.1)T^*_f + (11.4 \pm 2.3)C^*_{H_2} - (5.5 \pm 2.1)\beta^* - (6.2 \pm 2.2)C^*_{H_2} \cdot T^*_f \quad (5)$$

$$S_{Ni} = (44.3 \pm 2.0) + (12.4 \pm 2.4)F^*_{H_2} - (5.1 \pm 2.1)T^*_f + (11.4 \pm 2.3)C^*_{H_2} - (5.5 \pm 2.1)\beta^* - (6.2 \pm 2.2)\beta^* \cdot F^*_{H_2} \quad (6)$$

The difference between Eqs. (5) and (6) are the terms $C^*_{H_2} \cdot T^*_f$ and $\beta^* \cdot F^*_{H_2}$, which are equal over the experimental design matrix (Table 2). As made previously, three new experiments were designed and performed in order to maximize the differences of the two rival interactions over the experimental domain. Results obtained are presented in Table 6. If model predictions are compared, it is possible to notice that the model including the interaction term $\beta^* \cdot F^*_{H_2}$ (Eq. (6)) shows better performance. Fig. 3 shows the excellent agreement obtained between the experimental data and the model responses. An attempt to optimize the reduction conditions to this precursor shows that the optimum reduction condition is placed at the experimental condition 3 of the original experimental

Table 6
Experiments for selection of the significant interactions in Eqs. (5) and (6)

Number	Reduction	S_{Ni} (m^2/g Ni)			%R
		Eq. (5) prediction	Eq. (6) prediction	Experimental	
13	$15R_{1123\text{-}50\text{-}1.7}$	40.9	28.5	32.9	95.6
14	$15R_{873\text{-}50\text{-}10}$	73.9	61.5	63.0	100.0
15	$15R_{873\text{-}20\text{-}1.7}$	13.9	26.3	20.0	55.6

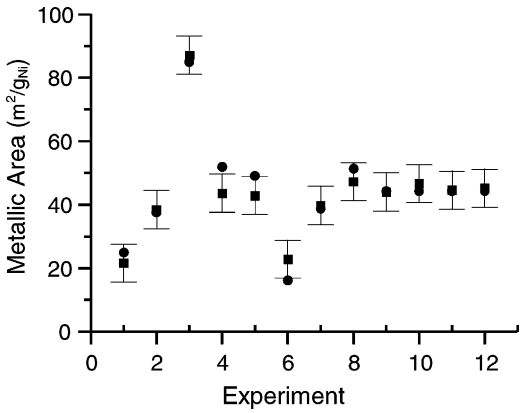

Fig. 3. Comparison between observed (■) and predicted metallic area (●) for the aged $40Ni_{363\text{-}363\text{-}20}$ precursor.

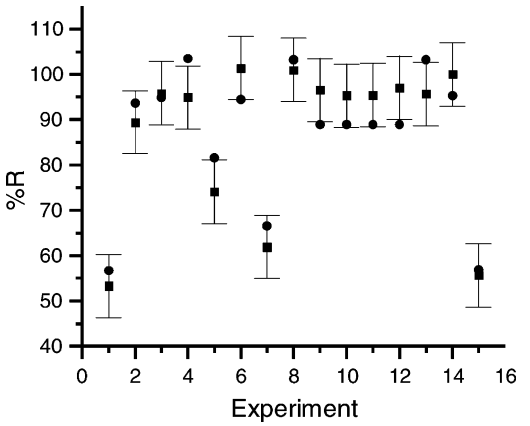

Fig. 4. Comparison between observed (■) and predicted degree of reduction (●) for the aged $40Ni_{363\text{-}363\text{-}20}$ precursor.

design matrix in Table 2 ($\beta^* = -1$, $F^*_{H_2} = +1$, $T^*_f = -1$ and $C^*_{H_2} = +1$). Hereafter, this condition will be called R_{Sil}, At these conditions, Table 4 shows that the experimental metallic area obtained experimentally was equal to $S_{Ni} = 87.1\,m^2/g$ Ni about 80% larger than the second best result obtained for experimental condition 8 ($S_{Ni} = 47.3\,m^2/g$ Ni).

When all experiments presented in Tables 4 and 6 are used to build a model for the degree of reduction of the aged precursor, then Eq. (7) is obtained as,

$$\%R = (87.5 \pm 2.1) + (11.4 \pm 2.3)T^*_f + (7.1 \pm 2.3)C^*_{H_2} + (51 \pm 2.3)F^*_{H_2} + -(7.3 \pm 2.3)C^*_{H_2} \cdot T^*_f \quad (7)$$

The degree of reduction is the final conversion of the reaction between the reducible species present in the catalyst and hydrogen. Thus, the effects of the reducing conditions on the degree of reduction are related to the increase of the reduction rate. The effects of the reduction temperature and hydrogen concentration upon the degree of reduction are in accordance with the expected trend, as reduction rates are expected to increase with the increase of temperature and of hydrogen concentration. The negative interaction between these two variables shows that the effect of the hydrogen concentration decreases as the reduction temperature decreases and that the apparent reaction order may be lower than one. The effect of the gas flow rate is probably related to the water removal from the reaction, as the hydrogen concentration is kept at higher values when the flow rate is higher. The quality of the fitting can be regarded as excellent, as it can be observed in Fig. 4.

The ultimate goal of this study was to establish optimum reduction recipes for high loading nickel silica catalyst prepared by the DP method. Thus, in order to test the optimized reduction procedures, two catalysts with very high metallic area per gram of reduced nickel were selected. Precipitation and aging conditions were set in accordance with the optimum values presented in a previous study [14]. The precursors and respective degrees of reduction, metallic areas per gram of nickel (S_{Ni}) and metallic areas per gram of reduced nickel (S'_{Ni}) are shown in Table 7 for the reducing conditions used in the previous study. Table 8 shows results obtained for the optimized reducing conditions presented here. Both optimized reducing conditions R_{Ox} and R_{Sil} were applied for both precursors.

For the $20Ni_{363\text{-}298\text{-}0}$ precursor, an increase of 70% in the metallic area is observed when the condition R_{Ox} is used for reduction, while the more severe R_{Sil} condition leads only to a marginal increase of the metallic

Table 7
Characterization of the two optimum catalyst precursors [14]

Precursor	Experimental		
	%R	S_{Ni} (m^2/g Ni)	S'_{Ni} (m^2/g Ni)
$20Ni_{363\text{-}298\text{-}0}$	81	60	73
$20Ni_{363\text{-}363\text{-}20}$	24	18	73

Table 8
Experimental R_{Ox} and R_{Sil} for optimum precursors

Precursor	Reduction condition	S_{Ni} (m^2/g Ni)	%R
$20Ni_{363\text{-}298\text{-}0}$	R_{Ox}	101.9	101
	R_{Sil}	65.5	100
$20Ni_{363\text{-}363\text{-}20}$	R_{Ox}	45.1	20
	R_{Sil}	58.7	86

area. As this precursor was not aged, it was composed mostly of nickel oxide. Therefore, the reducing conditions R_{Ox} are more appropriate to reduce it. Both reduction conditions were able to reduce the catalyst completely.

For the $20Ni_{363\text{-}393\text{-}20}$ precursor, a very significant increases of both metallic area and degree of reduction were observed when the R_{Sil} condition was used for reduction. For the other reduction condition, the observed increase of metallic area was smaller and the degree of reduction decreased. Since this catalyst was aged and a significant amount of silicate was present, it was no surprise that the R_{Sil} condition was more suitable for its activation.

Even though the R_{Sil} reduction condition allowed a significant increase of the metallic area of the $20Ni_{363\text{-}363\text{-}20}$ precursor, it seems that this was caused mostly by the increase of the amount of nickel reduced, as it can be inferred from the increase of the degree of reduction. A new attempt to increase the metallic area of this precursor was then performed. The TPR profile of this precursor (Fig. 5) shows that approximately 33% of the hydrogen uptake occurs in the same range of the $40Ni_{363\text{-}363\text{-}0}$ precursor

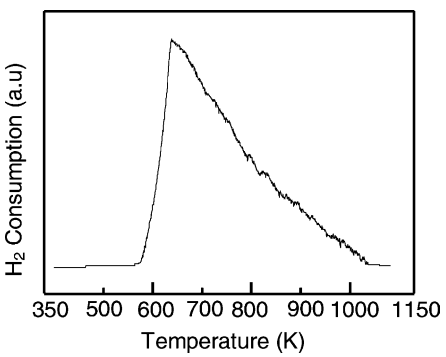

Fig. 5. TPR profile of the $20Ni_{363\text{-}363\text{-}20}$ precursor ($\beta = 5$ K/min, $C_{H_2} = 1.7\%$, $F_{H_2} = 50\ cm^3$/min and $T_f = 1150$ K).

(573–723 K), while the remaining hydrogen uptake occurs in the temperature range above 723 K. This suggests that approximately one-third of the nickel present in the $20Ni_{363\text{-}363\text{-}20}$ precursor is in the form of nickel oxide and that the remaining two thirds of nickel is in the form of silicate. Based on this additional piece of information regarding the relative amount of each reducible phase present in the precursor, a new reduction condition was designed to maximize the metallic area of both precursors.

The hydrogen concentration and the gas flow rate were found to affect only the metallic area of the $40Ni_{363\text{-}363\text{-}20}$ precursor (Eq. (6)) and therefore, should be set at their higher levels to maximize the metallic area. The heating rate influences both precursors, but in opposite directions. However, the influence of the heating rate is higher in the $40Ni_{363\text{-}363\text{-}20}$ precursor. In this case, a low heating rate should be used to obtain the maximum metallic area. Similar reasoning was used for the reduction temperature. In this case, the minimum reduction temperature in the experimental design (773 K) should be used. The results obtained at these operation conditions, however, were disappointing ($S_{Ni} = 31.8\ m^2$/g Ni, $\%R = 23.4$ at $\beta = 5$ K/min, $C_{H_2} = 10\%$, $F_{H_2} = 50$ ml/min and $T_f = 773$ K), as the metallic area decreased and the degree of reduction remained about 20%.

If an intermediate reduction temperature is calculated by weighing the amount of each phase present in the $20Ni_{363\text{-}363\text{-}20}$ precursor and assuming that the final reduction temperature had to remain in the lower level, in accordance with Eqs. (4) and (6), then the following empirical relation can be written,

$$T_{f(20Ni_{363\text{-}363\text{-}20})} = \tfrac{1}{3} T_f(-1)_{(40Ni_{363\text{-}363\text{-}0})} + \tfrac{2}{3} T_f(-1)_{(40Ni_{363\text{-}363\text{-}20})} = 835\ \text{K} \quad (8)$$

In this case, the final metallic area and the degree of reduction obtained for the $20Ni_{363\text{-}363\text{-}20}$ precursor were $65.9\ m^2$/g Ni and 87% (at $\beta = 5$ K/min, $C_{H_2} = 10\%$, $F_{H_2} = 50$ ml/min and $T_f = 815$ K). Therefore, the metallic area obtained at the new reducing conditions was significantly higher (around 12%) than the metallic area obtained previously with the optimized R_{Sil} condition. This seems to indicate that the reduction conditions may be optimized as functions of the

specific characteristics of the catalyst precursor, based on simple mathematical models built to describe the behavior of model catalyst precursors.

4. Conclusions

Statistical design of experiments was used to evaluate the relative importance of the operational variables and optimize the reduction step of the preparation of high loading Ni/SiO_2 catalysts. Two precursors with significantly different levels of nickel–support interaction were used and the relative importance of the operational variables and the optimum reduction conditions for each precursor (to maximize the degree of reduction and the metallic area of the final catalyst) were different showing that the proper procedure for catalyst activation depends strongly on the extent of the catalyst metal–support interaction.

For the precursor with low nickel–support interaction, formed predominantly by supported NiO, the degree of reduction was not sensitive to the reducing conditions within the experimental range analyzed. However, the final metallic area depended strongly on the operation conditions. Reduction at $\beta^* = +1$, $F^*_{H_2} = +1$ and $T^*_f = -1$ led to the maximum metallic area ($S_{Ni} = 33.8\,m^2/g$ Ni) within the range analyzed and allowed an increase of 70% of the metallic area for a similar precursor prepared in a previous study.

For the precursor with high nickel-support interaction, formed predominantly by nickel silicate, both the metallic area and the degree of reduction were found to be very sensitive to the operation conditions. The most important variable to describe the degree of reduction was the final reduction temperature because nickel silicate can only be reduced at high temperatures. The most important variables to describe the metallic area were the flow rate and the hydrogen concentration of the reducing mixture, in order to guarantee a more efficient water removal from the system. Reduction at $\beta^* = +1$, $F^*_{H_2} = +1$, $T^*_f = -1$ led to the maximum metallic area ($S_{Ni} = 87.1\,m^2/g$ Ni) within experimental the range analyzed and allowed an increase of the metallic area for a intermediate precursor prepared in a previous study ($S_{Ni} = 65.9\,m^2/g$ Ni and $\%R = 87$ instead of $S_{Ni} = 18.0\,m^2/g$ Ni and $\%R = 24$). In this particular case, optimum conditions were found through the linear combination of the empirical models developed for each model precursor ($Ni_{363\text{-}363\text{-}0}$ and $Ni_{363\text{-}363\text{-}20}$) analyzed, as the precursor previously prepared contained significant amounts of both NiO and silicate. This seems to indicate that the reduction conditions may be optimized as functions of the specific characteristics of the catalyst precursor, based on simple mathematical models built to describe the behavior of model catalyst precursors.

Acknowledgements

The authors thank Coordenação de Aperfeiçoamento de Pessoal de Nível Superior (CAPES) and Conselho Nacional de Desenvolvimento Científico e Tecnológico (CNPq) for providing scholarships and supporting this work.

References

[1] G.C.A. Schuit, L.L. van Reijen, Advances in Catalysis, Academic Press, New York, 1958.
[2] J.W.E. Coenen, B.G. Linsen, in: B.G. Linsen (Ed.), Physical and Chemical Aspects of Adsorbents and Catalysts, Academic Press, New York, 1970.
[3] J.W. Geus, J.A. Van Dillen, A.M. Hermans, et al., in: Proceedings of the Sixth International Congress on Catalysis, London, 1976.
[4] A.M. Hermans, J.W. Geus, in: B. Delmon, G. Poncelet, P.A. Jacobs (Eds.), Preparation of Catalysts II, Elsevier, Amsterdam, 1979, p. 113.
[5] F.F. Castillon, N. Bodganchikova, S. Fuentes, Appl. Catal. A 175 (1998) 55.
[6] N. Nakamura, R. Takahashi, S. Sato, T. Sodesawa, S. Yoshida, Phys. Chem. Chem. Phys. 2 (2000) 4983.
[7] P. Burattin, C. Louis, M. Che, J. Chem. Phys. 92 (1995) 1377.
[8] P. Burattin, M. Che, C. Louis, J. Phys. Chem. B 102 (1998) 2722.
[9] W.H. Wang, Y. Tang, J.B. Xiao, W.M. Hua, N. He, Z. Gao, Chem. Lett. 3 (2000) 282.
[10] V.M.M. Salim, M. Schmal, R. Frety, M.M. Rodrigues, M.S. Silveira, in: Reprints of the Fifth Brazilian Seminar on Catalysis, IBP, Guarujá, 1989, p. 93.
[11] A.F. da Silva Jr., V.M.M. Salim, M. Schmal, M.A.I. Duarte, R. Frety, in: B. Delmon, G. Poncelet, P.A. Jacobs (Eds.), Preparation of Catalysts V, Elsevier, Amsterdam, 1991.
[12] V.M.M. Salim, D.V. Cesar, M. Schmal, M.A.I. Duarte, R. Frety, in: B. Delmon, G. Poncelet, P.A. Jacobs (Eds.), Preparation of Catalysts VI, Elsevier, Amsterdam, 1995, p. 1017.
[13] C.C. Augusto, C.A. Perez, H.S. Amorim, L.C. Dieguez, V.M.M. Salim, in: Reprints of the Eighth Brazilian Seminar on Catalysis, IBP, Nova Friburgo, 1995.

[14] M. Nele, A. Vidal, D.L. Bhering, J.C. Pinto, V.M.M. Salim, Appl. Catal. A 178 (1999) 177.
[15] M. González, O. Gutiérrez, O.E. González, J.A. Delgaldo, J.R.G. Velasco, Appl. Catal. A 162 (1997) 269.
[16] M. González, O. Gutiérrez, O.E. González, J.R.G. Velasco, J. Mol. Catal. A 120 (1997) 185.
[17] A. Gil, A. Díaz, L.M. Gandía, M. Montes, Appl. Catal. A 109 (1994) 167.
[18] M. Che, Z.X. Cheng, C. Louis, J. Am. Chem. Soc. 117 (1995) 2008.
[19] P. Burattin, M. Che, C. Louis, J. Phys. Chem. B 104 (2000) 10482.
[20] G.E.P. Box, W.G. Hunter, J.S. Hunter, Statistics for Experimenters, Wiley, New York, 1978.
[21] A. Jones, B.D. McNicol, Temperature-Programmed Reduction for Solids Materials Characterization, Marcel Dekker, New York, 1986.
[22] J.W.E. Coenen, in: B. Delmon, G. Poncelet, P.A. Jacobs (Eds.), Preparation of Catalysts, Elsevier, Amsterdam, 1977, p. 89.